Forecasting the Maintenance of Quasi-Linear Mesoscale Convective Systems

MICHAEL C. CONIGLIO

Cooperative Institute for Mesoscale Meteorological Studies, University of Oklahoma, and NOAA/OAR/National Severe Storms Laboratory, Norman, Oklahoma

HAROLD E. BROOKS

NOAA/OAR/National Severe Storms Laboratory, Norman, Oklahoma

STEVEN J. WEISS AND STEPHEN F. CORFIDI

NOAA/Storm Prediction Center, Norman, Oklahoma

(Manuscript received 12 December 2005, in final form 12 September 2006)

ABSTRACT

The problem of forecasting the maintenance of mesoscale convective systems (MCSs) is investigated through an examination of observed proximity soundings. Furthermore, environmental variables that are statistically different between mature and weakening MCSs are input into a logistic regression procedure to develop probabilistic guidance on MCS maintenance, focusing on warm-season quasi-linear systems that persist for several hours. Between the mature and weakening MCSs, shear vector magnitudes over very deep layers are the best discriminators among hundreds of kinematic and thermodynamic variables. An analysis of the shear profiles reveals that the shear component perpendicular to MCS motion (usually parallel to the leading line) accounts for much of this difference in low levels and the shear component parallel to MCS motion accounts for much of this difference in mid- to upper levels. The lapse rates over a significant portion of the convective cloud layer, the convective available potential energy, and the deep-layer mean wind speed are also very good discriminators and collectively provide a high level of discrimination between the mature and dissipation soundings as revealed by linear discriminant analysis. Probabilistic equations developed from these variables used with short-term numerical model output show utility in forecasting the transition of an MCS with a solid line of 50+ dBZ echoes to a more disorganized system with unsteady changes in structure and propagation. This study shows that empirical forecast tools based on environmental relationships still have the potential to provide forecasters with improved information on the qualitative characteristics of MCS structure and longevity. This is especially important since the current and near-term value added by explicit numerical forecasts of convection is still uncertain.

1. Introduction

Forecasting the details of mesoscale convective systems (MCSs; Zipser 1982) continues to be a difficult problem. Recent advances in numerical weather prediction models and computing power have allowed for explicit real-time prediction of MCSs over the past few years (Done et al. 2004; Kain et al. 2005). While these forecasts are promising, their utility and how to best use their capabilities in support of operations is unclear (Kain et al. 2005). Therefore, refining our knowledge of the interactions of MCSs with their environment remains central to advancing our near-term ability to forecast MCSs.

Predicting MCS maintenance is fraught with challenges such as understanding how deep convection is sustained through system–environment interactions (Weisman and Rotunno 2004; Parker and Johnson 2004a,b; Coniglio et al. 2006a), how preexisting mesoscale features influence the systems (Fritsch and Forbes 2001; Trier and Davis 2005), and how the system itself can alter the inflow environment and feed back to

Corresponding author address: Dr. Michael C. Coniglio, National Weather Center, NSSL/FRDD, 120 David L. Boren Blvd., Norman, OK 73072.
E-mail: michael.coniglio@noaa.gov

DOI: 10.1175/WAF1006.1

changes in the system structure and longevity (Parker and Johnson 2004c; Fovell et al. 2005).

Evans and Doswell (2001) provide observational evidence that the strength of the mean wind (0–6 km) and its effects on cold pool development and MCS motion play a role in sustaining long-lived forward-propagating MCSs that produce damaging surface winds (derechos) through modifying the inflow of unstable air. They also show that a wide range of convective available potential energy (CAPE) and vertical wind shear is found in the environments of derechos, likely reflecting the variety of forcing mechanisms present in the spectrum of cases.

Through the use of wind profiler observations and numerical model output, Gale et al. (2002) examine nocturnal MCSs to determine predictors of their dissipation. Similar to Evans and Doswell (2001), they find that changes in the MCS's speed may control its dissipation through changes in low-level storm-relative inflow. However, despite some indications that a decreasing low-level jet intensity and low-level equivalent potential temperature (θ_e), and its advection, can be useful in some cases, they did not find robust predictors of MCS dissipation.

An analysis of derecho proximity soundings in Coniglio et al. (2004) shows that, as in Evans and Doswell (2001), CAPE and low-level wind shear vary considerably in derecho environments. Coniglio et al. (2004) also emphasizes that significant wind shear often exists in the mid- and upper levels in the preconvective environment. An emphasis of this work is that wind shear over deeper layers than those considered in past idealized modeling studies may be important for the maintenance of these systems. Stensrud et al. (2005) echo this result and suggest that this is especially true when the cold pool is very strong. This point may be particularly important because observations from the Bow Echoes and Mesoscale Convective Vortex (MCV) Experiment (BAMEX[1]) field campaign suggest that cold pools often extend to 3–5 km above ground (Bryan et al. 2005), which is deeper than cold pools in idealized simulations of convective systems (Coniglio and Stensrud 2001; Weisman and Rotunno 2004).

The goals of this work are to examine a large dataset of observed proximity soundings to identify predictors of MCS dissipation and to improve our understanding of MCS environments. The ultimate goal is to develop forecast tools that provide probabilistic guidance on the maintenance of MCSs. The focus is on the 3–12-h time scale, which could benefit Day 1 Severe Weather Outlooks, Mesoscale Discussions, and the issuance of Severe Weather Watches at the Storm Prediction Center (SPC), and short-term forecasts issued by local National Weather Service forecast offices.

The approach is to use statistical techniques (described in section 2) to identify the best predictors of MCS dissipation and use these predictors to develop an equation for the conditional probability of a strong, mature MCS. This study focuses on the robust systems that obtain a linear or curved leading line (which we will hereafter refer to as "quasi-linear") and tend to produce severe weather. Furthermore, the intention is to focus on systems that are driven primarily by cold pool processes and not those in which the dynamics are complicated by the presence of larger-scale external forcing (Fritsch and Forbes 2001; Trier and Davis 2005). The best predictors of MCS dissipation are discussed in section 3. Included in this section is a brief summary of some recent ideas on the importance of cold pool–deep shear environment interactions on MCS maintenance and how it relates to the current findings. Section 4 introduces the MCS probability equation and illustrates its potential utility. A summary and final discussion are given in section 5.

2. Data gathering and processing

a. MCS proximity soundings

To develop a large dataset of MCS proximity soundings, MCSs are identified by examining composites of base radar reflectivity for the months of May–August during the 7-yr period of 1998–2004. We follow the Parker and Johnson (2000) description of MCSs and focus our attention on the type that have a nearly contiguous quasi-linear or bowed leading edge of reflectivity values of at least 35 dBZ at least 100 km in length. Although a 100-km-long collection of cells could be considered an MCS if it persists for 2–3 h (Cotton et al. 1989), we only consider events that maintained this spatial configuration for at least five continuous hours to focus on the longer-lived events. From a set of over 600 MCSs of this type, we identified 269 events in which a radiosonde observation was taken within about 200 km and 3 h of the leading edge of the MCS and displayed no obvious signs of contamination from convection. In addition, only those soundings that appeared to be in the inflow environment are included in this tally. We add 79 derecho proximity soundings that were identified using a similar procedure in Coniglio et al. (2004)

[1] BAMEX was a field program designed to obtain high-density kinematic and thermodynamic observations in and around bow-echo MCSs and mesoscale convective vortices (Davis et al. 2004).

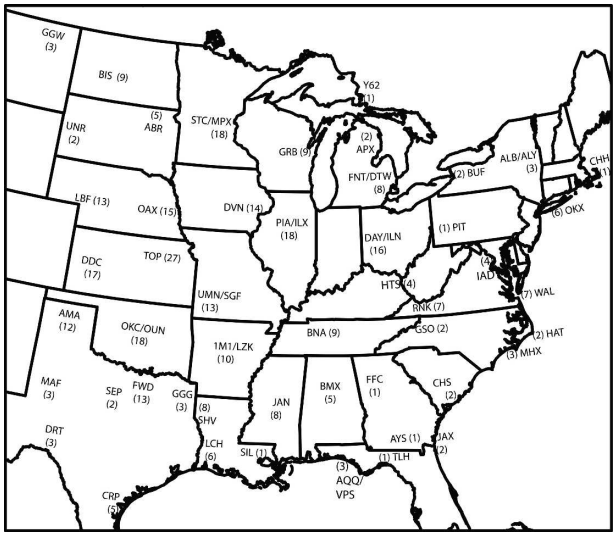

FIG. 1. The number and locations of soundings used in this study.

to amass a set of 348 warm-season (May–August) MCS proximity soundings[2] (Fig. 1).

At the time of the proximity sounding, the appearance and trends of the radar reflectivity are used to assess the mean speed and direction of the leading-line MCS motion and the stage of the MCS in its life cycle. The motion is defined by averaging the motions observed along the line at several points at a given time, then averaging these values in a 3-h window centered at the time of the sounding. Within this 3-h window, the stage of the MCS in its life cycle is defined as one of three stages: 1) initial cells prior to MCS development ("initiation"); 2) a mature MCS, with strengthening or quasi-steady high reflectivity (50 dBZ or higher) embedded within the nearly contiguous line of 35+ dBZ echoes ("mature"); and 3) a weakening MCS, with significantly weakened or shrinking areas of high reflectivity or a loss of system organization and associated areas of high reflectivity without any later reintensification ("dissipation").

The predictors for MCS maintenance are identified from a subset of MCSs in which the leading line was moving $\geq$10 m s^{-1} near the sounding time. Although MCSs that move at speeds of less than 10 m s^{-1} are not necessarily physically distinct from faster-moving systems, this helps to remove back-building and quasi-stationary systems. This produces a subset of 290 soundings that are used in the identification of the MCS maintenance predictors. These soundings are then stratified into 79 initiation, 96 mature, and 115 dissipation soundings based on the appearance and trends of the radar reflectivity at the time of the sounding as described above.

b. Identification of predictors

Several hundred variables are calculated from the soundings that represent various aspects of the kinematic and thermodynamic environment. We focus on a subset of variables that are found to have the largest statistically significant differences among the MCS categories (the "best predictors") while focusing on those variables that are often used by forecasters. The statistical procedure used to identify the best discriminators and the development of the forecast tool are described next [we refer the reader to Wilks (1995) for details on the components of the procedure].

To assess the significance of the differences, we use the Mann–Whitney test to identify variables that give the lowest probabilities (largest Z scores) that the population "locations" (the nonparametric analog to the mean) between the two groups in question are the same. Nonparametric tests like the Mann–Whitney test are appropriate in applications with relatively small datasets since there is no requirement to assume an underlying distribution to the data sample as required in the widely used Student's t test. Furthermore, the procedure allows one to use the Gaussian distribution on the Mann–Whitney test statistic to assess the confidence in the differences, even though the parent dataset may not be Gaussian (see Wilks 1995 for details). In the investigation of the predictors, we do not restrict the investigation to a handful of variables over a few layers but rather take a "brute force" approach by calculating various mean wind and wind shear variables over all possible layers $\geq$1 km deep up to 12 km and compute several versions of CAPE and instability measures that require vertical differentiation (lapse rates, bulk shear, etc.) over multiple layers. We then use the absolute magnitude of the Z scores to compare each variable between the mature and dissipation soundings to identify the particular kinematic and instability variables that are the most different between the two groups. In doing so, we use the property that the significance of the differences between the two groups is directly related to the magnitude of the Z score (the larger the Z score, the more significant the difference).

[2] This dataset is much more heavily weighted to high plains events than the derecho-only dataset of Evans and Doswell (2001) (cf. Fig. 1 and their Fig. 3). For example, 25% (86 out of 348) of our soundings are in the central and northern plains region west of the Missouri River, whereas only 5% (6 out of 113) of Evans and Doswell's soundings are found in this region. This disparity in the geographical distribution of the soundings should be noted if one attempts to compare and interpret the results of both studies.

For example, a Z score of 1.96 (2.58) corresponds to a 95% (99%) confidence that the "locations" of the two distributions in space (or the mean in a parametric test) are different in a two-tailed hypothesis testing approach.

Using the Z scores as a guide, linear discriminant analyses are then used to find the number and particular combination of variables that provide the best separation between the two groups in question. This amounts to determining the combination of variables that produces the highest percentage of correctly grouped soundings in a discriminant analysis. As detailed later, we find that the percentage of correct groupings converges to 1%–2% after the inclusion of only four variables in the analyses, which is a reflection of the substantial mutual correlations among the variables.

c. Logistic regression

Once the best predictors are identified, logistic regression[3] is used to develop an equation that gives the probability of one of the two groups occurring. Logistic regression is a method of producing probability forecasts on a set of binary data (i.e., data within two groups) by fitting predictors to the equation:

$$y = \frac{1}{1 + \exp(b_0 + b_1x_1 + b_2x_2 + \cdots + b_kx_k)}, \quad (1)$$

where the outputted y value is between one of the two binary data values, k is the number of predictors, x_k refers to the kth predictor, and b_k refers to the kth regression coefficient for each predictor. If the two input binary data values for the two groups are 0 and 1, then y becomes the fractional probability ($0 < y < 1$) of one of the groups occurring. This explains why logistic regression is fitting in this context because the resultant predictand is a probability; that is, it allows for the direct computation of probabilities between two possible outcomes in a set of data, which in this case is either a mature or a dissipating MCS.

The logistic regression equation is designed primarily to give the probability of a mature MCS as defined above, conditional on the development of an MCS. However, a consequence of the experimental design is that the predicted stage of the MCS is not independent of the predicted intensity of the MCS. This is because many of the same variables that discriminate well between the mature and weakening stages of a particular MCS also appear to discriminate well between MCSs of different intensities (Cohen et al. 2006). For example, large versus small CAPE could mean a mature versus a weakening MCS *and* a strong versus weak MCS. Therefore, the higher the probability of MCS maintenance, the more likely it is that an MCS will be maintained *and* be strong in a given environment, but the relative contribution to MCS maintenance compared to MCS intensity cannot be determined solely from the predictors in a particular case. We believe that this ambiguity in interpretation, however, does not hinder the general application of these ideas for the particular forecast problem of MCS maintenance, as we will show next.

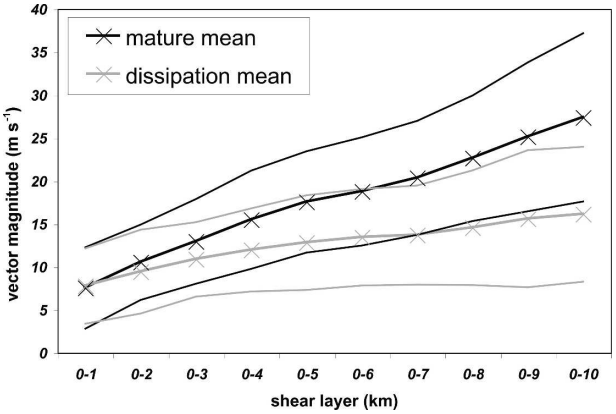

FIG. 2. Mean shear vector magnitudes (lines marked X) calculated over various depths among the mature (black) and dissipation (gray) sounding groups. The thin lines enclose ±1 std dev for the means.

3. Best kinematic predictors

a. Mean wind shear

Although many of the differences of the wind shear variables (shear vector magnitudes, total shear, positive shear, etc.) between the mature and dissipation soundings are large, the greatest differences, as gauged by the Z scores, are among the shear vector magnitudes (SVMs)[4] over very deep layers (Fig. 2). Figure 2 is produced with forecasters in mind who often use SVMs as a primary component in predicting the mode and severity of convection. This figure suggests that if the SVM is used as a shear metric, then is it better to look at deep layers versus shallow layers to forecast the weakening of MCSs. Indeed, the Z scores for the deep-layer shear values are very large (5.0–8.0), whereas the Z scores for the low-level shear values are much smaller

[3] We used the S-plus, version 6.1, software (http://www.insightful.com/support/doc_splus_win.asp) to perform the logistic regression.

[4] To clarify, the magnitude of the vector difference between the wind vectors at two different heights is defined to be the shear vector magnitude and is given in units of m s^{-1}.

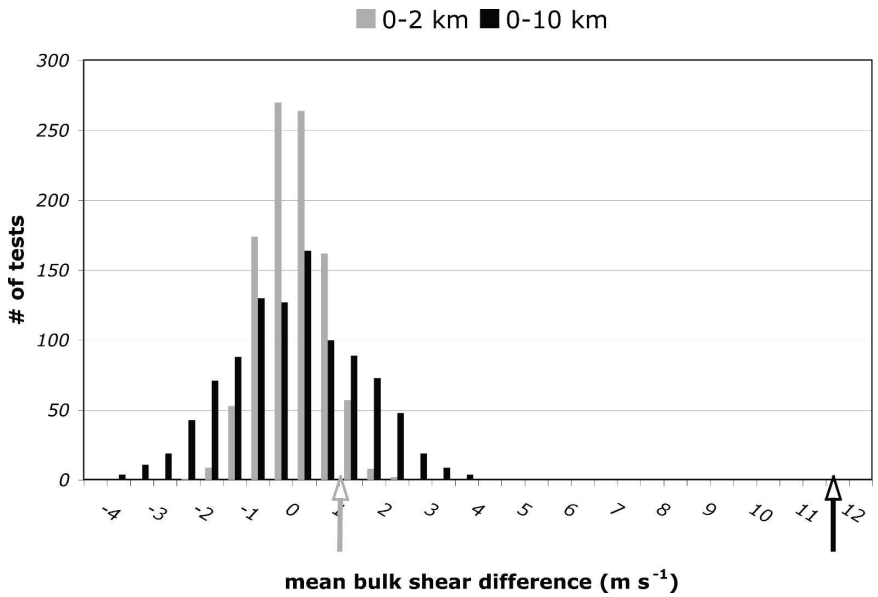

FIG. 3. Histogram of 1000 differences for the 0–2- (gray bars) and 0–10-km (black bars) shears between two random samples drawn from the 96 mature and 115 dissipation soundings. The gray arrow represents the 0–2-km shear difference between the mature and dissipation soundings (1.1 m s^{-1}) and the black arrow represents the 0–10-km shear difference between the mature and dissipation soundings (11.7 m s^{-1}). This illustrates that, while there is only about a 5% possibility that the 0–2-km shear is larger for the mature soundings by chance, there is virtually no possibility that the 0–10-km shear is larger for the mature soundings by chance and illustrates the much larger confidence in assessing differences between the mature and dissipation soundings using the 0–10-km shear compared to using the 0–2-km shear.

(1.0–2.0) (not shown). In fact, the deep-layer SVMs have the largest Z scores of *any* variables tested. The SVMs are larger for the mature soundings (Fig. 2) as suggested for derecho-producing MCSs alone (Coniglio et al. 2004). The differences in the low-level SVMs are relatively small, suggesting that these values, alone, have limited utility in determining the stage of the MCS life cycle.

To verify this further, a statistical resampling technique is applied to the dataset as follows: a random sample of 96 soundings is drawn from the set of 211 soundings that comprises the mature and dissipation soundings. The means of the 0–2-km SVM and the 0–10-km SVM are calculated for the 96 random soundings in the first group and for the 115 random soundings in the other group. The individual means are then differenced to obtain a mean 0–2-km SVM difference and a mean 0–10-km SVM difference in the random groups. This procedure is then repeated 1000 times. A histogram of the differences is displayed in Fig. 3 along with the 0–2-km SVM difference and the 0–10-km SVM difference between the original 96 mature and 115 dissipation soundings. It is found that 52 out of the 1000 random draws produced a 0–2-km SVM difference larger than the 0–2-km SVM difference between the mature and dissipation soundings (1.1 m s^{-1}). This suggests that there is about a 5% possibility that the 0–2-km SVM is larger for the mature soundings by chance. While this in itself is a good result statistically, a comparison of the results for the 0–10-km SVMs shows that none of the 0–10-km SVMs for the random draws were greater than the mature versus dissipation difference. In fact, the 11.7 m s^{-1} difference for the 0–10-km SVMs between the mature and dissipation soundings *is almost 3 times larger than the largest difference obtained in the random draws* (4.05 m s^{-1}) (Fig. 3). In other words, there is virtually no possibility that the difference between the 0–10-km SVM between the mature and dissipation soundings was obtained by chance and the improvement from using the 0–10-km SVM over the 0–2-km SVM is about threefold.

A closer inspection of the shear profiles between the mature and dissipation soundings sheds light on the kinematic reasons for this result (Figs. 4–6). The shear profile [$\partial V_s(z)$ in units of s^{-1}] shows that the mean shear is greater for the mature soundings at every vertical level (Fig. 4). Therefore, it seems that a measure that integrates these differences over a large depth should be beneficial.

Judging by the Z scores in Fig. 4, these differences

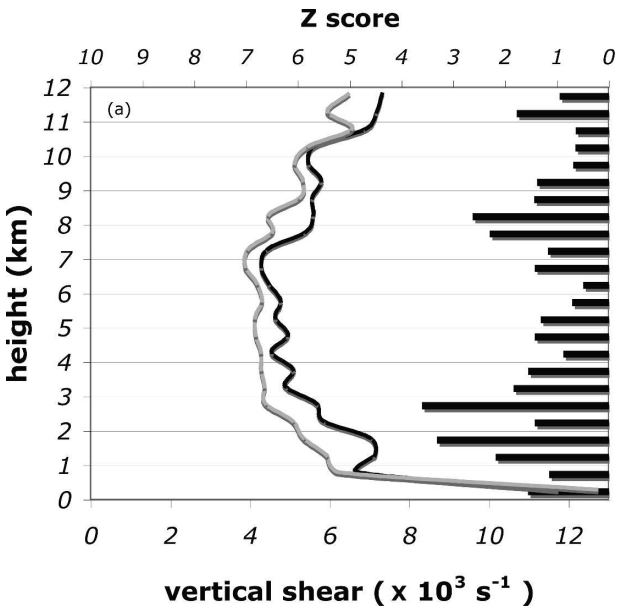

FIG. 4. Mean shear profile calculated every 500 m for the mature (black line) and dissipation (gray line) soundings as a function of height AGL. The horizontal bars on the right side of the figure display the *Z* score (using the *x* axis at the top of the figure) for the differences in the shear between the mature and dissipation soundings at each vertical level.

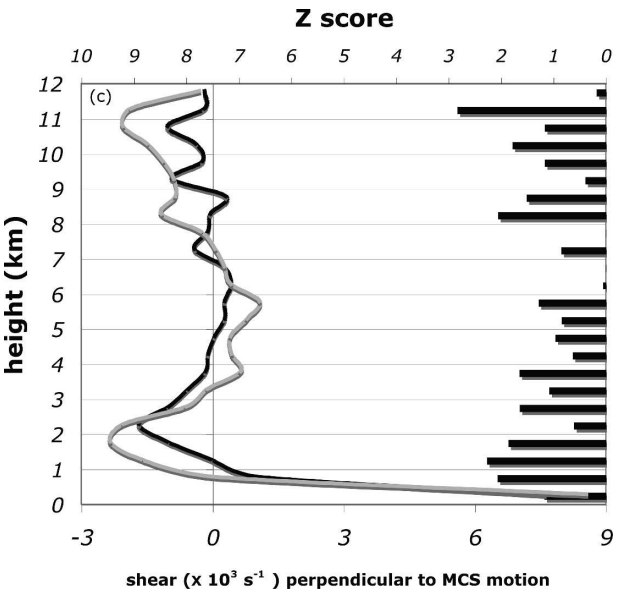

FIG. 6. As in Fig. 4 but for the mean shear profile perpendicular to MCS motion (which is usually nearly parallel to the MCS leading line).

are most significant between 2–3 km and near 8 km. An inspection of the shear components in MCS motion-relative coordinates helps elucidate how the shear is contributing to these differences (Figs. 5 and 6). This is important to examine because the orientation of the shear and its vertical distribution play a key role in the longevity and organizational characteristics of MCSs (Weisman et al. 1988; Parker and Johnson 2004c; Coniglio et al. 2006a). It is clear that the mean component of the shear *parallel* to MCS motion [$\partial u_s(z)$], which is usually nearly perpendicular to the MCS leading line, is greater at all levels for the mature soundings, except very close to the ground and near the tropopause. Judging by the *Z* scores in Fig. 5, these differences are most significant at 1–2 km and especially at 6–9 km, in which the mean MCS motion-parallel shear for the mature soundings is nearly triple what it is for the dissipation soundings.

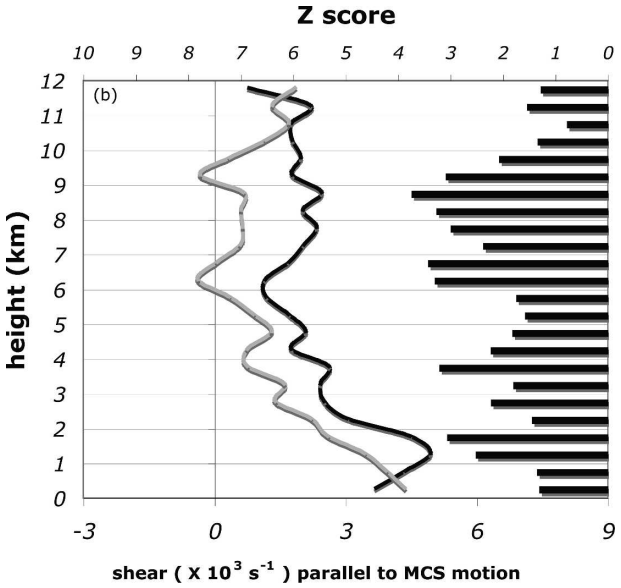

FIG. 5. As in Fig. 4 but for the mean shear profile parallel to MCS motion (which is usually nearly perpendicular to the MCS leading line).

Looking at low levels first, by viewing the mean component of shear *perpendicular* to MCS motion [$\partial v_s(z)$], which is usually nearly parallel to the leading line, we see that the larger $\partial V_s(z)$ seen in the 1–2-km layer for the mature soundings (Fig. 4) has a contribution from a larger positive $\partial u_s(z)$ for the mature soundings (Fig. 5), but also has a contribution from a larger *negative* magnitude of $\partial v_s(z)$ for the dissipation soundings (Fig. 6). The contributions from $\partial u_s(z)$ in the 1–2-km layer are probably related physically to the organizational benefits of positive low-level line-perpendicular shear (Parker and Johnson 2004c; Weisman and Rotunno 2004). The increase in negative line-parallel shear for the dissipation soundings is likely related to a decrease in the southerly relative inflow component at 2–3 km (an inspection of these wind components verifies this

claim). Collectively, Figs. 4–6 illustrate that the low-level SVMs represent differences in shear that are important in both the line-perpendicular and line-parallel directions.

Looking at the upper levels, the larger $\partial V_s(z)$ for the mature soundings (Fig. 4) is much more apparent when viewing the mean MCS motion-parallel shear (Fig. 5), in which the Z scores are >3 (corresponding to a $>99\%$ confidence in the statistical differences) for most levels between 6 and 9 km. The larger shear is almost entirely due to the larger $\partial u_s(z)$ (Fig. 5) since $\partial v_s(z)$ is nearly identical at 6–8 km between the two groups (Fig. 6). There are indications though that $\partial v_s(z)$ does become important above 8 km as the values become larger and negative for the dissipation soundings. The most important point here though is that the possible physical benefits to mature MCSs related to a larger upper-level shear component parallel to MCS motion are revealed in Fig. 5. Since this feature of MCS environments has been given little attention in the literature compared to low-level shear (Weisman and Rotunno 2004), we briefly review some recent ideas on how this upper-level line-normal shear can benefit mature MCSs.

1) Cold pool–wind shear interactions

For many years, researchers have employed idealized convection-resolving numerical models to understand the physical importance of the environmental low-level wind shear in countering the effects of the cold pool and controlling the behavior of quasi-linear MCSs (see Weisman and Rotunno 2004 for a review). Studies on the physical effects of deeper shear on MCSs are scarcer, but have been appearing more frequently in recent literature (Shapiro 1992; Fovell and Daily 1995; Moncrieff and Liu 1999; Coniglio and Stensrud 2001; Parker and Johnson 2004a,b,c; Coniglio et al. 2006a). In particular, numerical simulations in Parker and Johnson (2004c) show that in deep shear environments, convective updrafts interact with the positive shear to generate pressure perturbations that accelerate the flow downshear in mid- and upper levels (this concept is illustrated in Fig. 7). These transient pressure perturbations account for a significant portion of the net overturning of unstable air over time. As in some analytical studies of 2D convection (Shapiro 1992; Moncrieff and Liu 1999), it is hypothesized that the deeper shear gives parcels more upright trajectories and allows them to accelerate upward for longer periods.

This model of deep convective overturning in deep shear is examined further in Coniglio et al. (2006a) through idealized 3D numerical simulations of convective systems in varying amounts of vertical shear in the 5–10-km layer above a fixed amount of low-level shear

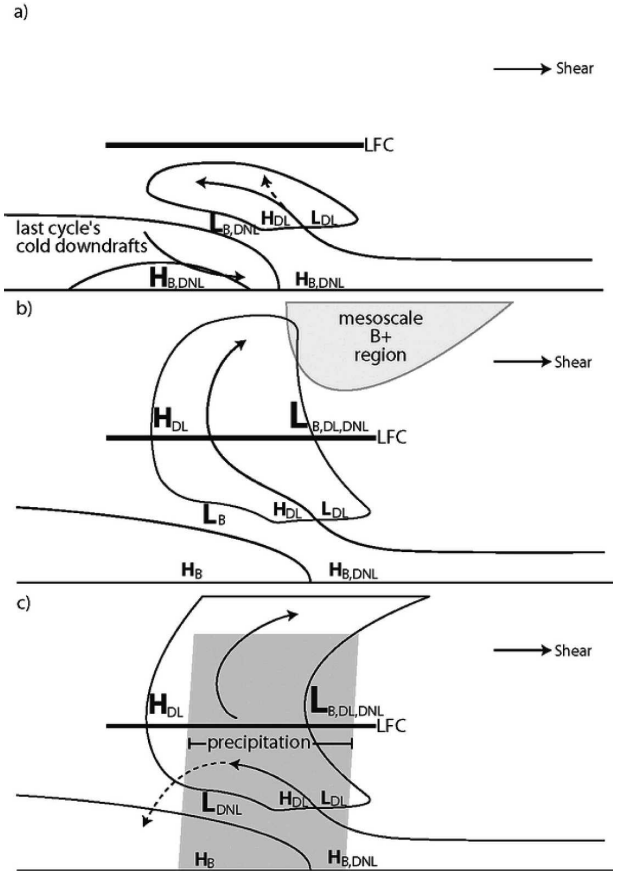

FIG. 7. Schematic depiction of a multicellular cycle within a convective system in deep shear. (a) Development of a fresh updraft at the outflow boundary–gust front. (b) Maturation of the overturning updraft. (c) The updraft is cut off from the inflow by precipitation. The cold pool and cloud outlines are shown schematically, along with typical airstreams. The LFC and orientation of the deep tropospheric shear vector are also shown. In (b), the shaded region represents the mesoscale region of positive buoyancy associated with the line-leading cloudiness. In (c), the shaded region represents the newly developed convective precipitation cascade. Pressure maxima and minima are shown with the letters H and L, respectively; their sizes indicate approximate magnitudes and their subscripts indicate the pressure components to which they are attributed [buoyancy (B), dynamic linear (DL), and dynamic nonlinear (DNL)]. The vertical scale is expanded somewhat below the LFC and contracted somewhat above the LFC (from Parker and Johnson 2004b).

[20 m s^{-1}(0–5 km)$^{-1}$]. They show quantitatively that the addition of shear in the 5–10-km layer can allow for much deeper lifting of the overturning air parcels and a much greater percentage of parcels that are lifted to higher levels (Fig. 8). They argue that the deeper shear facilitates the development of a steering level (the level at which the cold pool speed matches the line-normal environmental wind speed) somewhere in mid- and upper levels. This allows the favorable downshear accel-

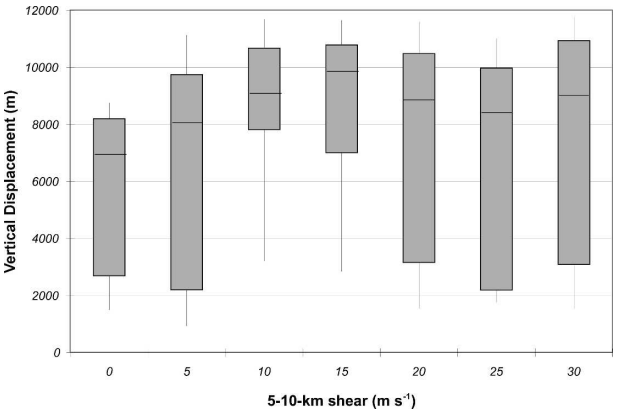

FIG. 8. Distributions of the maximum vertical displacements of several hundred parcels that pass through the deep convective regions of simulated convective systems within various values of the 5–10-km shear (all of the simulations have a fixed-value wind speed difference of 20 m s^{-1} over 0–5 km). The lines extend to the 10th and 90th percentiles and the boxes enclose the interquartile range (25th and 75th percentiles). The thin lines within each box represent the median (from Coniglio et al. 2006a).

erations shown in Fig. 7 to keep the convective regions close to the cold pool leading edge, which facilitates the maintenance of the system as a whole. An emphasis of this work is that parcels above 1 km are responsible for the deep overturning in these deeper shear regimes and the lifting is maximized for moderate upper-level shear values [10–15 m s^{-1} $(5–10\ km)^{-1}$; Fig. 8)]. The benefit of the deeper lifting is manifest in quasi-2D regimes as larger, stronger, more upright collections of line segments and bow echoes that persist along the leading edge of the cold pool and is also apparent in 3D regimes with mixed-mode convective systems.

2) SUMMARY OF WIND SHEAR RESULTS

The recent studies mentioned above suggest that physical mechanisms related to upper-level shear are relevant to both quasi-2D and -3D regimes of MCSs and that the low-level shear–cold pool interactions that can help determine the strength and structure of the systems initially (Weisman and Rotunno 2004) do not provide a complete picture of the complex question of MCS structure and maintenance. This may be especially true once a strong, organized cold pool and deep mesoscale updrafts become established above a surface stable layer. The present results reflect this perspective since the SVM over a very deep layer is shown to be a much better discriminator as compared to the low-level SVMs. This is likely because of the significant influence that mid- to upper-level wind shear can have on the maintenance of MCSs along with the positive influences of the low-level shear on the initial organization and strength of the system (Weisman and Rotunno 2004). Equivalently, the results from Figs. 2–4 suggest that *an integrated measure of shear over a very deep layer has the most utility in forecasting the weakening of quasi-linear MCSs*. Calculations of the total shear, or the hodograph length, which are correlated to the SVMs, support this claim (not shown).

Although we have focused on the 0–10-km shear because it has the largest Z score among all of the variables, it is desirable to include a shear predictor in the logistic regression procedure that accounts for the possibility of variable heights of the lower- or upper-level jets that can control the effective depth and magnitude of the deep-layer shear. Therefore, we define the "maximum deep shear" to be the maximum SVM between any wind vector in the lowest 1 km and any wind vector in the 6–10-km layer. The Z score for the maximum deep shear is slightly smaller than that for the 0–10-km shear, but still very large relative to the shallower shear.

b. Mean wind speeds

In addition to the deep-layer wind shear, the deep-layer mean wind speeds are very different between the mature and dissipation soundings. The 3–12-km mean wind speed has the largest Z score among the mean wind variables and is a large improvement over using a low-level-only mean wind (e.g., 0–6 km) (this is verified by a resampling technique similar to that produced for the wind shear variables). The 3–12-km mean wind speed is therefore used in the logistic regression procedure. An examination of the mean wind speed profile reveals that the winds in upper levels contribute the most to this discrimination (Fig. 9). Specifically, notice in Fig. 9 that the mean wind speeds are greater for the mature soundings than the dissipation soundings at 99% confidence ($Z > 2.65$) at all levels above 5 km, and the confidence only increases with height up to 12 km. Inspection of the synoptic-scale flow patterns shows that this decrease in upper-level wind speeds for dissipating MCSs can usually be attributed in large part to the background flow in which the systems often propagate away from the upper-level features and associated jet streams that contributed to their initiation and maturity (Coniglio et al. 2004) (this also applies to decreases in upper-level shear as MCSs dissipate).

In the discriminant analyses described in the next section, the mean wind does not improve the discrimination substantially because of a moderate linear correlation with the maximum deep shear values. However, the inclusion of the mean winds allows for the possibility of representing environments that can support MCSs through mean wind–cold pool interactions

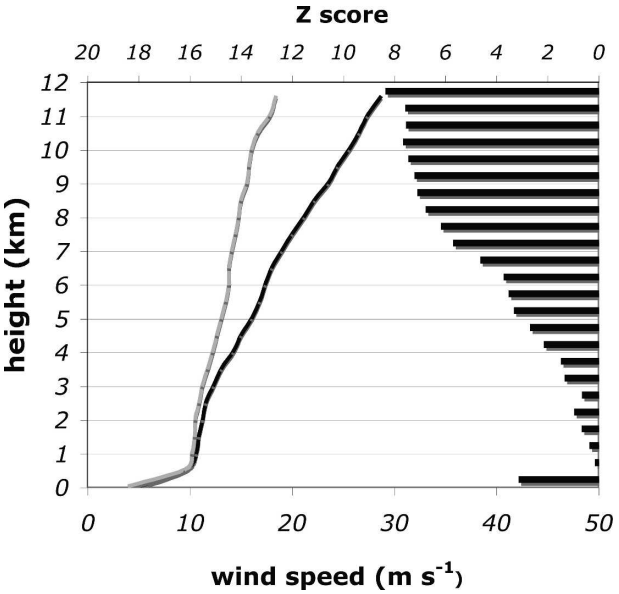

FIG. 9. As in Fig. 4 but for the mean wind speed.

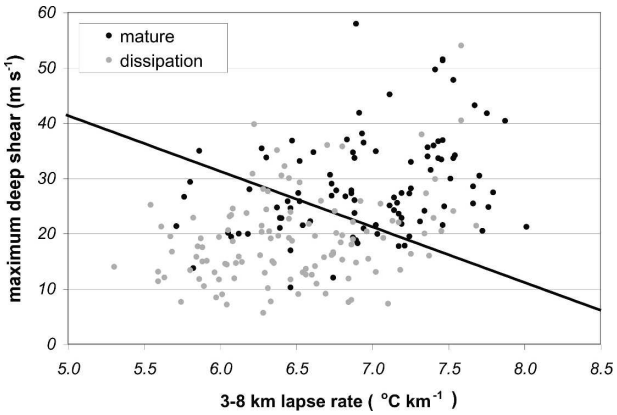

FIG. 10. Scatterplot of the maximum deep shear (m s^{-1}) vs the 3–8-km lapse rate (°C km^{-1}) for the mature and dissipation soundings. The linear discrimination line separates 75% of the soundings correctly.

(Evans and Doswell 2001; Corfidi 2003) in strong wind–weak shear environments.[5] These environments appear to be more common to the MCS events that occur over the eastern third of the United States in our dataset, although the relatively small sample size for these events prevents a definitive statement on this possible regional characteristic.

c. Thermodynamic variables

Using similar procedures as described above, we examine many thermodynamic variables related to instability including, but not limited to, several variations of CAPE, lapse rates over many layers, and vertical differences in equivalent potential temperature (θ_e) over many layers. We find that the mean lapse rates over a deep portion of the convective cloud layer (generally from the lifting condensation level to some level in the 500–300-hPa layer) are the most different among the mature and dissipation soundings. Although it is not surprising that larger lapse rates are found for stronger, more mature MCSs, the physical importance of the deeper midlevel lapse rates versus the lower-level lapse rates is not obvious. One hypothesis is that steeper midlevel lapse rates make it easier for the shear in the convective cloud layer to maintain upright trajectories by allowing the convective updrafts to reach their vertical velocity potential earlier in the overturning process, as related to the processes described in section 3b. This could lead to more cells that unload their precipitation close to the leading edge of the gust front compared to systems that occur in a smaller midlevel lapse rate environment. The 3–8-km lapse rate has the highest Z score among the two groups and is much better than using a low-level-only lapse rate (e.g., 1–4 km), as verified by resampling, and is thus used as the primary instability variable in the logistic regression procedure.

A discriminant analysis between the two groups shows that the 3–8-km lapse rate, along with the maximum deep shear, separate 75% of the mature and dissipation soundings correctly (Fig. 10), which illustrates the potential utility of the deep shear and lapse rates in this context. Figure 10 clearly demonstrates that strong, mature MCSs generally persist in the larger deep shear, larger lapse rate portion of the parameter space and MCSs generally dissipate under the weaker deep shear, smaller lapse rate portion of the spectrum. However, several outliers are present that do not fit the overall pattern and it is instructive to briefly examine their characteristics. An examination of five mature soundings found in the lower-left corner of Fig. 10 reveals recurring features, such as large surface-based CAPE (>3500 J kg^{-1}), very high equilibrium levels (ELs; 14–16 km AGL), very little convective inhibition (CIN) in which the lifting condensation level (LCL) ≅ the level of free convection (LFC), and high relative humidity from the surface to 500 hPa. In addition, all but one case have very low lifting condensation levels (LCLs) (~600–800 m) (the exception was a sounding from Dodge City, Kansas, taken in a deep well-mixed boundary layer). In these environments, large parcel buoy-

[5] It is important to recognize that the shear–cold pool interactions ultimately control the structure of the systems, but the effects of topography and surface friction and their effects on convergence along the cold pool may become important for fast-moving systems.

ancy (governed by the lapse rates) and shear apparently become unnecessary to retrigger and organize convection along the cold pool, or any other linear forcing mechanism, given the relative ease with which parcels can rise nearly undiluted to the high EL.

A similar inspection of MCSs that dissipate despite large 3–8-km lapse rates and large maximum shear values (from the upper-right corner of Fig. 10) does not reveal a multitude of obvious similarities among the outliers, and potential reasons for the dissipation seem to vary from case to case. For example, the obvious outlier in Fig. 10 with a lapse rate ≈ 7.6 K km^{-1} and shear ≈ 54 m s^{-1} occurred on 2 May under unseasonably strong synoptic-scale forcing and the dissipation was coincident with the squall line outrunning the frontal convergence. Another system had its inflow contaminated by a cold pool remaining from a mesoscale region of light rain from earlier in the day shortly after the sounding was taken. In another case, the system became oriented parallel to the shear precluding the further organization of a progressive linear system. Therefore, while MCSs that persist despite small lapse rates and deep shear may perhaps be identifiable by the vertical distribution of the thermodynamic properties of the sounding, it is not as obvious that dissipating MCSs in large lapse rates and deep shear can be anticipated as easily and is a limitation of this approach.

Among the other thermodynamic variables, we find that various CAPEs that are based on finding the most unstable mixed parcel over some layer tend to have large Z scores between the mature and dissipation soundings and, interestingly, are only weakly correlated with the 3–8-km lapse rates. A similar lack of a strong relationship between CAPE and parcel instability (as measured by the lifted index) was shown by Blanchard (1998). The lack of a strong correlation in this study appears to be because the CAPE variables are determined largely by the absolute moisture content in the layer with the maximum θ_e rather than the vertical temperature profile and its control on parcel buoyancy. The use of a CAPE variable in the logistic regression that is not tied to a particular level is desirable because this preserves the ability to represent systems that may be sustained by elevated inflow. This also may allow some representation of MCSs that persist in "tall and thin" CAPE environments (Blanchard 1998), like those mentioned above, in which the lapse rates may not be large but the CAPE can still be significant if the equilibrium level pressure is very low. As illustrated in section 5, the probability equations are applied using Rapid Update Cycle (RUC; Benjamin et al. 2004) output. Therefore, we use the method of calculating the "best" CAPE in the RUC model as of this writing (hereafter denoted RCAPE) as another predictor in the logistic regression. In this method, if the parcel with the maximum θ_e is found in the lowest 70 hPa, the RCAPE is calculated from a mixed parcel in the lowest 70 hPa; otherwise, the single most unstable parcel is used to calculate the CAPE (D. Bright 2006, personal communication).

4. MCS maintenance probability equation

The four variables described above (maximum deep shear, 3–8-km lapse rate, RCAPE, 3–12-km mean wind speed) collectively separate over 80% of the soundings correctly when input into a linear discriminant analysis between the mature and dissipation soundings. It is worth noting that, because of the mutual correlations among the hundreds of variables, any additional variables provide negligible (<1%) improvement to the discrimination of the two groups. Therefore, the maximum deep shear (maxshear), 3–8-km lapse rate (3–8 lr), RCAPE, and 3–12-km mean wind (3–12 mw) are used as input to Eq. (1) to develop the MCS maintenance probability (MMP):

For RCAPE ≥ 100 J kg^{-1}:

$$\text{MMP} = \frac{1}{\langle 1 + \exp\{a_0 + [a_1(\text{maxshear})] + [a_2(\text{3–8 lr})] + [a_3(\text{RCAPE})] + [a_4(\text{3–12 mw})]\}\rangle} \tag{2}$$

For RCAPE < 100 J kg^{-1}:

$$\text{MMP} = 0,$$

where the regression coefficients are $a_0 = 13.0$ (dimensionless), $a_1 = -4.59 \times 10^{-2}$ m^{-1} s, $a_2 = -1.16$°C^{-1} km, $a_3 = -6.17 \times 10^{-4}$ J^{-1} kg, and $a_4 = -0.17$ m^{-1} s. Note that the MMP is set to zero for RCAPE values below 100 J kg^{-1} regardless of the values of the other predictors.

As illustrated in Fig. 11, if all four of the predictors obtain their median values in the combined mature and dissipation sounding dataset (maxshear = 21 m s^{-1}, 3–8 lr = 6.7°C^{-1} km, RCAPE = 1731 J kg^{-1}, 3–12 mw = 17 m s^{-1}), then the regression equation predicts an 85%

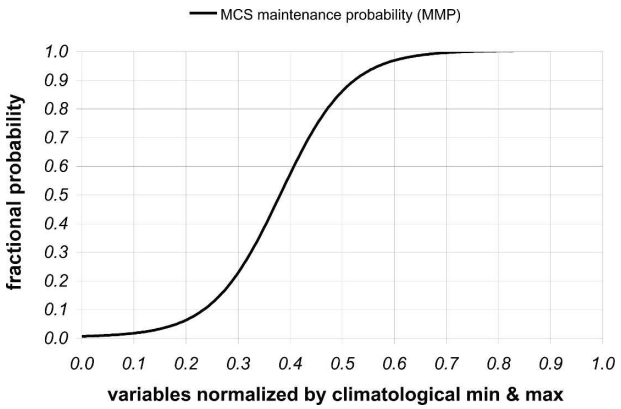

FIG. 11. Probability of MMP (solid line) based on logistic regression. The ordinate represents the predictors normalized by their minimum and maximum values in the data subset. For example, if all four of the predictors for the equation for MCS maintenance are exactly halfway between their minimum and maximum values (0.5), then the regression equation predicts an ~85% chance that the MCS will be strong and maintained. In dimensional values, this corresponds to a maximum deep shear of 21 m s^{-1}, a 3–8-km lapse rate of 6.7°C km^{-1}, an RCAPE of 1731 J kg^{-1}, and a 3–12-km mean wind speed of 17 m s^{-1}. In general, a steeper curve means a better ability of the parameter predictors to discriminate between the two groups.

chance[6] that the MCS will be strong and be maintained. The normalization of the variables in Fig. 11 is done to allow a smooth curve to be plotted so that the important point of the steepness of the curve for the MMP can be gained. In general, a steeper curve suggests a better ability to discriminate between the two groups and, therefore, the steepness of the curve suggests the potential for substantial skill in discriminating between mature and weakening MCSs.

Application of the MMP

We envision the best real-time application of the MMP would use observational data or short-term model output at a time close to convective initiation. For example, gridded fields from the hourly RUC can be used to calculate the probabilities and give guidance to the regions most likely to sustain strong MCSs that develop (this is illustrated later in this section). This could benefit Day 1 Severe Weather Outlooks, Mesoscale Discussions, and the issuance of Severe Weather Watches at the SPC, and short-term forecasts issued by local forecast offices.

[6] Note that this is only one of many ways that a probability of 85% can be reached depending on the values of the predictors. For example, one particular sounding in the dataset has maxshear = 42 m s^{-1}, 3–8 lr = 6.9°C km^{-1}, RCAPE = 383 J kg^{-1}, 3–12 mw = 21 m s^{-1}, and also has an MMP of 85%.

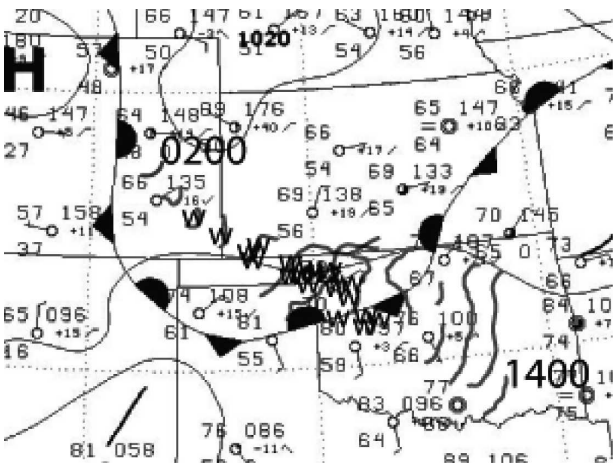

FIG. 12. Surface chart valid at 0600 UTC 1 Jul 2005 produced by the National Centers for Environmental Prediction. Solid gray lines denote the hourly positions of the leading edge of the 50+ dB*Z* echoes associated with the supercell and MCS from 0200 to 1400 UTC. The Ws denote locations of severe wind reports.

A small collaborative program recently took place during the summer of 2005 at the SPC and the National Severe Storms Laboratory (NSSL) as part of the National Oceanic Atmospheric Administration Hazardous Weather Testbed to test the ability of the MMP to provide useful guidance to forecasters at the SPC (visit the Web site http://www.nssl.noaa.gov/hwt/for more information). To meet the goals of this program, daily activities included the documentation of MCSs using national mosaic radar reflectivity and the evaluation of the probabilities calculated using the hourly RUC forecasts. An example of one of these cases and the application of the MMP are shown next.

1 JULY 2005 MCS

An application of the MMP is illustrated with an MCS event that occurred between 0000 and 1400 UTC on 1 July 2005 in the central and southern plains region (Fig. 12). A nearly stationary synoptic front meandered from the Front Range of the Colorado Rockies southward into far northeastern New Mexico, then stretched eastward across the Texas Panhandle, and eventually northeastward toward the central Mississippi River valley. Isolated convection developed in east-central Colorado during the late afternoon of 30 June and developed into an elevated supercell that moved through southeastern Colorado and southwestern Kansas from 0200 to 0500 UTC (Fig. 12). Although northeasterly surface winds were found up to ~750 hPa north of the front (not shown), the boundary layer was well mixed and supported convectively generated surface winds > 40 m s^{-1}. The supercell then grew upscale and devel-

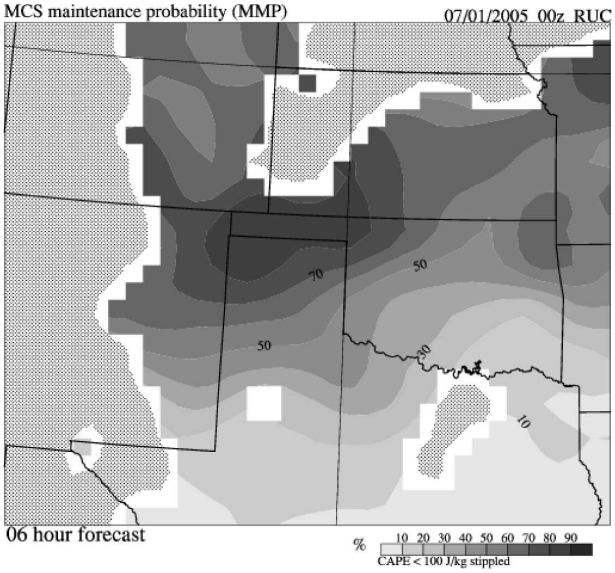

FIG. 13. MMP (%) based on a 6-h RUC forecast valid at 0600 UTC 1 Jul 2005. Hatched areas represent areas with CAPE < 100 J kg^{-1}.

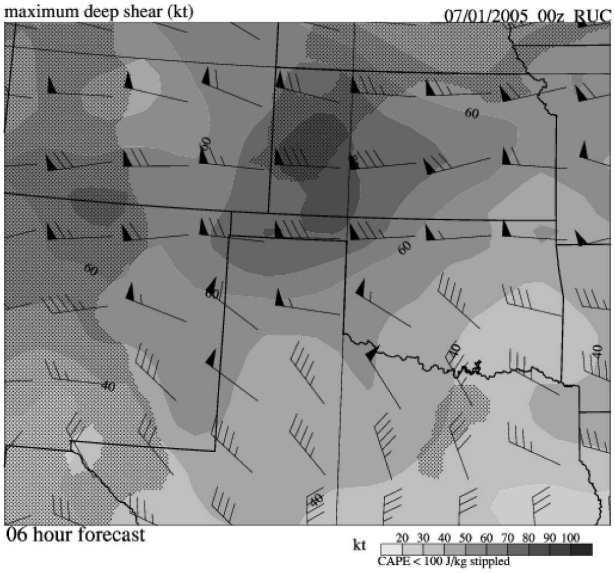

FIG. 14. Maximum bulk deep shear (kt) based on a 6-h RUC forecast valid at 0600 UTC 1 Jul 2005. Hatched areas represent areas with CAPE < 100 J kg^{-1}.

oped linear characteristics as it entered Oklahoma after 0600 UTC, with a continuation of the severe surface winds north of the front (Fig. 12).

Although forecasters were aware of the potential for severe thunderstorm winds in this region, the persistence and strength of the thunderstorm winds north of the front were not anticipated. It is intriguing that the MMP values are high (70%–90%) in the region where the supercell transitioned to an MCS in southwestern Kansas and northwestern Oklahoma (Fig. 13). From examining the components of the MMP (Figs. 14–17), it is evident that the maximum deep shear values of 70–80 kt and 3–8-km mean lapse rates over 7.5 K km^{-1} contributed most to the high probabilities, since the RCAPE values and the 3–12-km mean wind values are not particularly large (500–1500 J kg^{-1} and 35–40 kt, respectively). It is also intriguing that the area that experienced the severe surface winds was confined to the region of higher MMP values. This could have steered forecasters to examine this area for the potential for organized severe surface winds more critically, despite the location of the system well north of the front in a region of northeasterly low-level flow.

Just as important, and perhaps the more challenging aspect of the forecast, was the cessation of the severe surface winds and the weakening of the convective system once it entered the warm sector air (Fig. 12). The line underwent changes in structure to a more disorganized state and showed characteristics of discrete forward propagation as it crossed the frontal zone. The line then reorganized temporarily into a solid but weaker linear system before dissipating altogether in eastern Oklahoma by 1400 UTC (Fig. 12). Just as the MMP values could have increased the awareness of an organized severe wind threat in southwestern Kansas and far northwestern Oklahoma, the MMP values could have alerted forecasters to the rapidly decreasing probability of an organized system across central Okla-

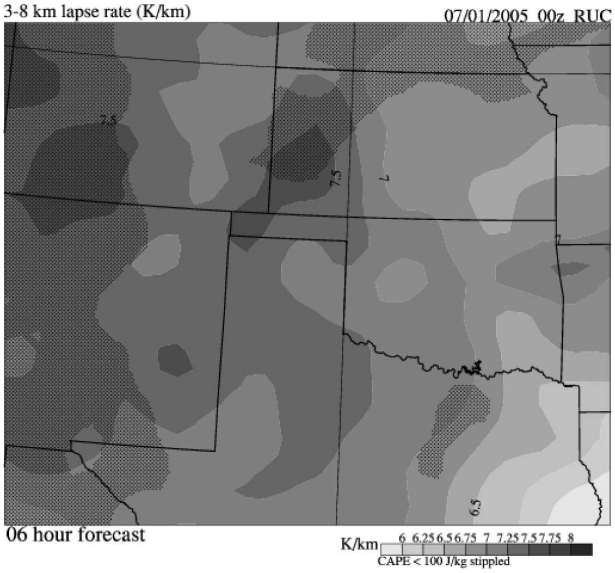

FIG. 15. The 3–8-km mean lapse rate (°C km^{-1}) based on a 6-h RUC forecast valid at 0600 UTC 1 Jul 2005. Hatched areas represent areas with CAPE < 100 J kg^{-1}.

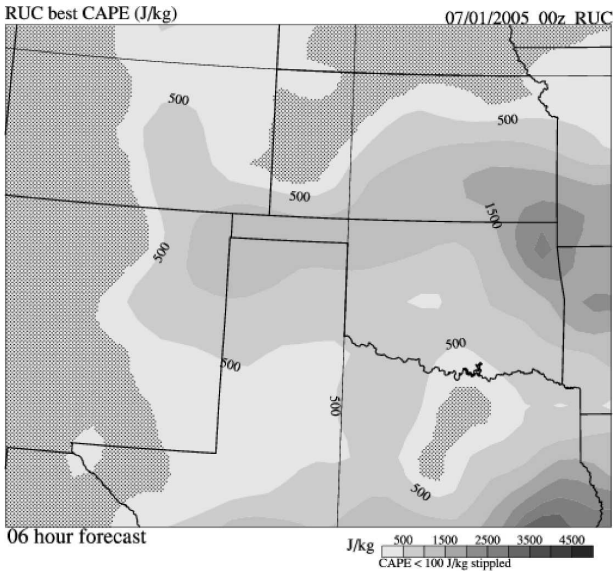

FIG. 16. RUC "best" CAPE (see text for description) based on a 6-h RUC forecast valid at 0600 UTC 1 Jul 2005. Hatched areas represent areas with CAPE < 100 J kg^{-1}.

homa with values dropping quickly to 20%–30% across this region (Fig. 13), despite the presence of an unstable and weakly capped warm-sector air mass. Although the 3–8-km lapse rates, the RCAPE values, and the 3–12-km mean wind speeds all show a decrease along the path of the system, a large gradient in maximum deep shear values that drop quickly from over 70 kt over the Oklahoma panhandle to less than 40 kt across west-central Oklahoma (Fig. 14) appears to be the primary reason for the rapid drop in the MMP.

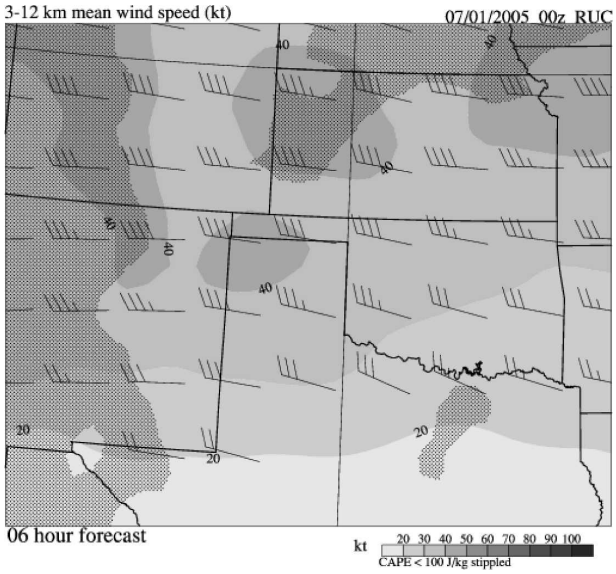

FIG. 17. The 3–12-km mean wind (kt) based on a 6-h RUC forecast valid at 0600 UTC 1 Jul 2005. Hatched areas represent areas with CAPE < 100 J kg^{-1}.

Although verification of the MMP is ongoing (see Coniglio et al. 2006b), the equations appear to satisfy the goals of this study by providing useful guidance on the transition of a system with a solid line of 50+ dBZ echoes to a more disorganized system with unsteady changes in structure and propagation characteristics, as in the above example. This speaks to the potential of the MMP to help in the MCS forecast problem, despite the ambiguity in the interpretation of the equation discussed earlier. More generally, this also speaks to the need for forecasters to look at the integration of sounding-derived parameters, such as the SVMs and the lapse rates, in forecasting the near-term behavior of quasi-linear MCSs. Finally, this brings into question the utility of using low-level-only parameters, including mean winds speeds, lapse rates, and, as detailed in Evans and Doswell (2001), Gale et al. (2002), Coniglio et al. (2006a), and in this paper, the low-level vertical shear.

5. Summary and discussion

This paper addresses the problem of predicting the maintenance of quasi-linear MCSs. Environmental variables that best differentiate between mature and weakening MCSs are identified from a large set of observed proximity soundings. The goal is to use these variables to develop a tool that provides probabilistic guidance on MCS maintenance. A fitting method of calculating probabilities in this context is logistic regression, which gives the probability of a strong, mature MCS in this application.

For the discrimination of mature and weakening MCS environments, the mean vertical wind shear over a very deep layer is found to be the variable with the largest statistical differences. An examination of the shear components reveals that larger MCS motion-parallel shear for the mature MCS environments contributes to this difference in the upper levels, whereas the differences in the low-level shear are related to both the MCS motion-parallel and -perpendicular shear components in the 1–3-km layer. Some possible physical mechanisms for this difference in upper-level shear and the importance of using a deep layer when assessing the shear are summarized in section 3. Mean lapse rates over a significant depth of the convective cloud, the maximum mixed-layer CAPE, and low-to-upper level mean wind speeds also discriminate between mature and weakening MCSs very well. The differences in the mean wind speeds are highly significant above 5 km and especially in the 7–12-km layer.

Early verification suggests that the logistic regression equation based on these predictors and used with short-term numerical model output can provide useful guidance on the transition of a system with a solid line of 50+ dB*Z* echoes to a more disorganized system with unsteady changes in structure and propagation characteristics. A more indirect, but equally useful, application may be on the potential for an MCS to produce severe surface winds on regional scales, although the skill of this application in a general sense remains to be seen.

We are also mindful of the limitations of this technique and, to that end, in the use of cold pool/shear concepts for the forecasting of MCSs in general. We have found that once MCSs become established, decreasing deeper-layer wind shear, mean wind speed, CAPE, and decreasing lapse rates in the lower half of the convective cloud layer appear to be excellent predictors of a weakening MCS. This appears to be especially true of the systems that mature in the larger deep-shear/larger lapse-rate regimes in the central United States during the warm season, as in the example shown at the end of section 4. We emphasize that these concepts will likely work best on MCSs that develop and continually generate strong cold pools away from strong larger-scale forcing when the shear and mean winds are substantial. However, MCSs can maintain coherence through other means, including discrete propagation along a surging outflow (one such case occurred with an MCS on 30 June 2005 in the Ohio Valley), frontogenetic circulations, low-level jet processes, gravity wave interactions, and other larger-scale forcing mechanisms, in which the probability equations may not be as applicable. Indeed, we observed several systems that persisted despite small mean lapse rates and deep-layer shear. These environments tend to be very moist with low LCLs, high ELs, little to no CIN, and large CAPEs. Regarding these other MCS modes, we will report on the overall performance of the equations documented for MCS cases in a future paper.

We remind the reader that the concepts developed in this paper are applied with the goals of the SPC in mind, particularly with the issuance of the day 1 convective outlooks and watches along MCS tracks. We recognize that the convective-scale details of the situation ultimately dictate the county-scale locations of severe surface winds. Accurate prediction at these scales likely will await advances in the ability to observe the finescale details of the low-level moisture and advances in the prediction of these systems with numerical weather prediction schemes that assimilate convective-scale observations (Dowell et al. 2004). But the concepts presented above illustrate that forecast tools based on environmental variables and their statistical relationships still have the potential to provide forecasters with improved information on the qualitative characteristics of MCS structure and longevity, and perhaps refined information on the potential for severe weather on regional scales. We urge the meteorological community to continue to undertake studies of this type to help improve mesoscale convective weather forecasting in the near term while we move forward into the era of convective-scale data assimilation using high-resolution numerical weather prediction models.

Acknowledgments. This paper was greatly improved by the thoughtful reviews by Dr. Chris Davis and an anonymous reviewer. We also thank Drs. Matt Parker and Robert Fovell for the helpful discussions regarding the background material for this paper. The SPC/NSSL 2005 Summer Program would not have been possible without the help of David Bright and Jay Liang of the SPC. We thank the SPC forecasters and the NSSL scientists who have volunteered their time to participate in the program. We are also grateful to Bob Johns for contributing his time and wealth of knowledge and experience to this project. The majority of this project was supported through a National Research Council Postdoctoral Award for the first author under the guidance of the second author. Funding for the latter stages of the project was provided by NOAA/Office of Oceanic and Atmospheric Research under NOAA–University of Oklahoma Cooperative Agreement NA17RJ1227, U.S. Department of Commerce.

REFERENCES

Benjamin, S. G., and Coauthors, 2004: An hourly assimilation–forecast cycle: The RUC. *Mon. Wea. Rev.,* **132,** 495–518.

Blanchard, D. O., 1998: Assessing the vertical distribution of convective available potential energy. *Wea. Forecasting,* **13,** 870–877.

Bryan, G., D. Ahijevych, C. A. Davis, and M. L. Weisman, 2005: Observations of cold pool properties in mesoscale convective systems during BAMEX. Preprints, *32d Conf. on Radar Meteorology and 11th Conf. on Mesoscale Processes,* Albuquerque, NM, Amer. Meteor. Soc., CD-ROM, JP5J.12.

Cohen, A. E., M. C. Coniglio, S. F. Corfidi, and S. J. Taylor, 2006: Discriminating among non severe, severe, and derecho-producing mesoscale convective system environments. Preprints, *Symp. on the Challenges of Severe Convective Storms,* Atlanta, GA, Amer. Meteor. Soc., CD-ROM, P1.15.

Coniglio, M. C., and D. J. Stensrud, 2001: Simulation of a progressive derecho using composite initial conditions. *Mon. Wea. Rev.,* **129,** 1593–1616.

——, ——, and M. B. Richman, 2004: An observational study of derecho-producing convective systems. *Wea. Forecasting,* **19,** 320–337.

——, ——, and L. J. Wicker, 2006a: Effects of upper-level shear on the structure and maintenance of strong quasi-linear mesoscale convective systems. *J. Atmos. Sci.,* **63,** 1231–1252.

——, M. Bardon, K. Virts, and S. J. Weiss, 2006b: Forecasting the maintenance of mesoscale convective systems. Preprints, *23d Conf. on Severe Local Storms,* St. Louis, MO, Amer. Meteor. Soc., CD-ROM, P2.3.

Corfidi, S. F., 2003: Cold pools and MCS propagation: Forecasting the motion of downwind-developing MCSs. *Wea. Forecasting,* **18,** 997–1017.

Cotton, W. R., M.-S. Lin, R. L. McAnelly, and C. J. Tremback, 1989: A composite model of mesoscale convective complexes. *Mon. Wea. Rev.,* **117,** 765–783.

Davis, C. A., and Coauthors, 2004: The Bow-Echo and MCV Experiment (BAMEX): Observations and opportunities. *Bull. Amer. Meteor. Soc.,* **85,** 1075–1093.

Done, J., C. A. Davis, and M. L. Weisman, 2004: The next generation of NWP: Explicit forecasts of convection using the Weather Research and Forecasting (WRF) model. *Atmos. Sci. Lett.,* **5,** 110–117.

Dowell, D. C., F. Zhang, L. J. Wicker, C. Snyder, and N. A. Crook, 2004: Wind and temperature retrievals in the 17 May 1981 Arcadia, Oklahoma, supercell: Ensemble Kalman filter experiments. *Mon. Wea. Rev.,* **132,** 1982–2005.

Evans, J. S., and C. A. Doswell, 2001: Examination of derecho environments using proximity soundings. *Wea. Forecasting,* **16,** 329–342.

Fovell, R. G., and P. S. Daily, 1995: The temporal behavior of numerically simulated multicell-type storms. Part I: Modes of behavior. *J. Atmos. Sci.,* **52,** 2073–2095.

——, B. Rubin-Oster, and S. Kim, 2005: A discretely propagating nocturnal Oklahoma squall line: Observations and numerical simulations. Preprints, *22d Conf. on Severe Local Storms,* Hyannis, MA, Amer. Meteor. Soc., CD-ROM, 6.1.

Fritsch, J. M., and G. S. Forbes, 2001: Mesoscale convective systems. *Severe Convective Storms, Meteor. Monogr.,* No. 50, Amer. Meteor. Soc., 323–357.

Gale, J. J., W. A. Gallus Jr., and K. A. Jungbluth, 2002: Toward improved prediction of mesoscale convective system dissipation. *Wea. Forecasting,* **17,** 856–872.

Kain, J. S., S. J. Weiss, M. E. Baldwin, G. W. Carbin, D. Bright, J. J. Levit, and J. A. Hart, 2005: Evaluating high-resolution configurations of the WRF model that are used to forecast severe convective weather: The 2005 SPC/NSSL Spring Experiment. Preprints, *21st Conf. on Weather Analysis and Forecasting and 17th Conf. on Numerical Weather Prediction,* Washington, DC, Amer. Meteor. Soc., CD-ROM, 2A.5.

Moncrieff, M. W., and C. Liu, 1999: Convection initiation by density currents: Role of convergence, shear, and dynamical organization. *Mon. Wea. Rev.,* **127,** 2455–2464.

Parker, M. D., and R. H. Johnson, 2000: Organizational modes of midlatitude mesoscale convective systems. *Mon. Wea. Rev.,* **128,** 3413–3436.

——, and ——, 2004a: Structures and dynamics of quasi-2D mesoscale convective systems. *J. Atmos. Sci.,* **61,** 545–567.

——, and ——, 2004b: Simulated convective lines with leading precipitation. Part I: Governing dynamics. *J. Atmos. Sci.,* **61,** 1637–1655.

——, and ——, 2004c: Simulated convective lines with leading precipitation. Part II: Evolution and maintenance. *J. Atmos. Sci.,* **61,** 1656–1673.

Shapiro, A., 1992: A hydrodynamical model of shear flow over semi-infinite barriers with application to density currents. *J. Atmos. Sci.,* **49,** 2293–2305.

Stensrud, D. J., M. C. Coniglio, R. Davies-Jones, and J. Evans, 2005: Comments on "'A theory for strong long-lived squall lines' revisted." *J. Atmos. Sci.,* **62,** 2989–2996.

Trier, S. B., and C. A. Davis, 2005: Propagating nocturnal convection within a 7-day WRF–model simulation. Preprints, *32d Conf. on Radar Meteorology and 11th Conf. on Mesoscale Processes,* Albuquerque, NM, Amer. Meteor. Soc., CD-ROM, P2M.1.

Weisman, M. L., and R. Rotunno, 2004: "A theory for strong long-lived squall lines" revisited. *J. Atmos. Sci.,* **61,** 361–382.

——, J. B. Klemp, and R. Rotunno, 1988: Structure and evolution of numerically simulated squall lines. *J. Atmos. Sci.,* **45,** 1990–2013.

Wilks, D. S., 1995: *Statistical Methods in the Atmospheric Sciences*. Academic Press, 467 pp.

Zipser, K. A., 1982: Use of a conceptual model of the life cycle of mesoscale convective systems to improve very-short-range forecasts. *Nowcasting,* K. Browning, Ed., Academic Press, 191–204.